Indian Journal of Chemical Technology
Vol. 32, January 2025, pp. 78-84
DOI: 10.56042/ijct.v32i1.5071

# Corrosion protection of mild steel substrates using silver nanoparticles synthesized from *Nicotiana tabacum* leaf extract

Preeti Jain[1]*, Jeetendra Bhawsar[2], Archana Lakhani[3] & Balram Patidar[1]

[1]Medi-Caps University, Indore, 453331, Madhya Pradesh-453 331, India

[2]Atal Bihari Vajpayee Hindi University, Bhopal, Madhya Pradesh-462 038, India

[3]UGC-DAE- Consortium for Scientific Research, Indore, Madhya Pradesh-453 331, India

*E-mail: preeti.jain@medicaps.ac.in

*Received 23 August 2023; accepted 5 December 2024*

A successful way to protect mild steel (MS) substrates from corrosion is described by using silver nanoparticles (Ag-NPs) synthesized by applying co-precipitation method using extract derived from *Nicotiana tabacum* leaves. Using a transmission electron microscope, a full morphological analysis was done and using X-ray diffraction average crystallite size is found to be 19.1 nm. Both 0.1 M hydrochloric acid (HCl) and 3.5% sodium chloride (NaCl) are used for determination of behaviour of mild steel substrates in corrosive environments. The anti-corrosive performance is evaluated via potentiodynamic polarization studies. In solutions of 0.1 M HCl and 3.5% NaCl, Ag NPs-coated substrates show very high corrosion efficiencies of 94.27% and 96.30%, respectively. To provide further insights into surface morphology, scanning electron microscopy is employed. This analysis underscores the excellent corrosion resistance achieved by implementing Ag-NPs.

**Keywords:** Anticorrosive, Corrosion protection, Mild steel, *Nicotiana tabacum* leaf extract, Silver nanoparticles

## Introduction

The deposition of nanoparticles (NPs) on metal surfaces is a versatile and promising technique for corrosion protection. Numerous studies have demonstrated the superior performance of NPs compared to bulk-sized materials due to their higher surface area-to-volume ratio, enhanced reactivity, and better adherence to substrates[1-3]. Consequently, researchers have increasingly focused on investigating nanomaterials for corrosion control, which provide safe and environmentally friendly methods for protecting metals[4,5]. Metals serve as structural pillars in numerous industries[6], but they are prone to degradation and corrosion when exposed to the surrounding environment, leading to a loss of essential qualities and diminished effectiveness and reliability in fulfilling their intended functions[7,8]. As a result, environmental corrosion of metals is a significant global challenge [9,10], with high costs associated with corrosion repair, highlighting the need for reliable and cost-effective protective techniques[11,12].

Recent advancements in nanotechnology have introduced innovative strategies for combating corrosion. For instance, nanomaterials such as graphene, carbon nanotubes, and metal oxide NPs have been explored for their ability to create robust and impermeable coatings[13]. Among these, silver nanoparticles (Ag-NPs) have emerged as a promising candidate due to their exceptional antimicrobial properties, high conductivity, and superior chemical stability[14]. However, despite extensive research on nanomaterials, there is a significant gap in understanding the specific corrosion protection mechanisms of Ag-NPs and their integration into coatings for long-term performance.

This research aims to develop anti-corrosion techniques utilizing Ag-NPs. The inclusion of Ag-NPs in the coating enhances barrier properties, providing dynamic protection and controlling the corrosion rate over an extended period. Additionally, nanomaterial coatings offer improved scratch resistance and adhesion to the surface[13,15]. The application of nanomaterials for corrosion protection has been extensively explored, and the use of Ag-NPs as a corrosion control agent represents a novel and pioneering endeavour.

This study stands as the first of its kind to delve into the corrosion potential inherently possessed by Ag-NPs. The incorporation of these NPs into coatings imparts not only enhanced barrier properties but also

the ability to dynamically regulate corrosion rates over prolonged periods. This innovative approach presents a departure from traditional corrosion mitigation strategies, introducing a fresh perspective that capitalizes on the unique attributes of Ag-NPs. The corrosion tests were conducted in 0.1 M hydrochloric acid (HCl) and 3.5% sodium chloride (NaCl) salt media. HCl is a common corrosive agent, and its presence in various industrial processes and environments can lead to significant material degradation. By subjecting the coated substrates to an acidic environment represented by 0.1 M HCl, the study aims to simulate conditions where corrosion risk is heightened. This is particularly relevant considering the widespread use of mild steel in industrial applications where exposure to acids is prevalent.

On the other hand, NaCl is the primary component of common salt, and its presence can lead to corrosion through saltwater exposure or other chloride-rich environments. The research can address issues that arise in marine environments, coastal installations, and other places where corrosion due to chloride is a major issue by using a 3.5% NaCl solution as a corrosive medium. The Ag-NPs were synthesized using a green synthesis method, and the coating was applied to the substrate through dip coating techniques. To assess the crystal size and morphology of the Ag-NPs, X-ray diffraction (XRD) and Transmission electron microscopy (TEM) techniques were used and the surface study of mild steel coupon was carried out using scanning electron microscopy (SEM). Corrosion rates were measured using potentiodynamic polarization experiments.

## Experimental Section

### Required Materials and Preparations

Silver nitrate ($AgNO_3$), sodium chloride (NaCl), and hydrochloric acid (HCl) were utilized for all experimental procedures and all the chemicals were purchased from Merck from S.D. Fine Chemicals Industry. Dry *Nicotiana tabacum* leaves were obtained from a local market. Freshly prepared double-distilled water, obtained using a lab-installed craft distillation unit, was used throughout the experiments.

To prepare the *Nicotiana tabacum* leaf extract, 10 g of dry leaves were soaked in 100 mL distilled water. The mixture was heated to 60°C and stirred continuously for 20 min. After cooling to room temperature, the mixture underwent filtration using Whatman filter paper and subsequent centrifugation for 20 min. The resulting extract was stored in the refrigerator for future use.

Next, the synthesis of Ag-NPs was carried out using a green method. A 0.1 M $AgNO_3$ precursor solution was combined with the *Nicotiana tabacum* leaf extract in a ratio of 1:10 v/v. The solutions were manually shaken and exposed to sunlight to facilitate the reduction process. This led to the formation of Ag-NPs, initially appearing whitish yellow and eventually turning dark red, which is a characteristic colour change observed in the reduction of colloidal silver[16-18].

The mechanism for the green synthesis of Ag-NPs involves the reduction of $Ag^+$ ions by the *Nicotiana tabacum* leaf extract, which acts as a natural reducing and capping agent. The bioactive compounds in the extract, such as flavonoids, phenols, and alkaloids, facilitate the reduction process. Upon exposure to sunlight, which serves as a catalytic energy source, the $Ag^+$ ions are reduced to metallic silver ($Ag^0$), as indicated by the colour change from whitish yellow to dark red. This approach leverages the dual role of the *Nicotiana tabacum* extract, ensuring the synthesis of stable and uniformly dispersed Ag-NPs.

For the deposition process, mild steel substrates with dimensions of 10 mm ×10 mm ×2 mm were prepared. The substrates were coated with epoxy resin and attached to conducting wires for the subsequent electrochemical experiment. A surface area of 10 mm ×10 mm was left exposed on the substrates. Prior to deposition, the substrates underwent grinding with 1200 FF emery papers and polishing with a 1 μm diamond paste. Ultrasonic cleaning with acetone was performed, followed by thorough drying of the substrates.

The cleaned mild steel substrates were directly immersed in a solution of Ag-NPs for 30 min to allow adsorption of the particles onto the surface. Subsequently, the substrates were dried and covered with aluminium foil before being placed in a dark environment for further experimentation.

### Morphological Study

#### *X-Ray Diffraction Study*

The XRD pattern of the prepared thin film of Ag-NPs was recorded using a D8 ADVANCE X-ray diffractometer. The diffractometer utilized Cu-Kα radiation with a wavelength (λ) of 1.5406 Å, operating at 40 kilovolts (kV) and 40 milliamperes

(mA) in the 2θ/θ scanning mode. The data acquisition covered a 2θ range of 10 to 90 degrees, with a small step size of 0.02 degrees between each measurement point. This allowed for a detailed analysis of the thin film. The thin film shows the diffraction pattern and the crystal structure of the Ag-NPs.

***Morphology of Ag-NPs***

The surface morphology of Ag-NPs including size, lattice image and shape was examined and recorded using Philips-CM200 Transmission Electron Microscope.

***Surface Morphology of Steel Coupons***

The surface morphology of mild steel coupons was comprehensively examined under six different conditions using a JEOL JSM-6390A Analytical Scanning Electron Microscope. This technique holds significant value in the examination of surface morphology[19,20]. This comprehensive analysis of the surface morphology provides crucial information for evaluating the effectiveness of the corrosion inhibition process and further optimizing the protective properties of the deposited Ag-NPs on the mild steel substrate.

**Potentiodynamic Polarization**

Electrochemical measurements were performed to evaluate the electrochemical properties of the synthesized Ag-NPs on the mild steel substrate. The measurements were carried out using a potentiostat in a three-electrode cell configuration. The Ag-NPs-coated mild steel substrate served as the working electrode, while a platinum electrode and a saturated calomel electrode (SCE) were used as the counter and reference electrodes, respectively. The electrolyte used for the measurements was 3.5% NaCl and 0.1 M HCl. The obtained data were analysed using Tafel extrapolation method to extract relevant electrochemical parameters such as corrosion potential, current, cathodic and anodic slopes.

## Results and Discussion

**Morphological Study**

***X-Ray Diffraction Study***

The XRD pattern is shown in Fig. 1 indicates the crystalline nature of the thin film[21]. The presence of different phases in the film was compared with the standard JCPDS data (File number 04-0783). The XRD data and its analysis are presented in Table 1. Notably, sharp peaks were observed at the (2 0 0), (2 2 0), and (2 2 2) planes, corresponding to Ag-NPs. The crystallite size of the Ag-NPs plays a significant role in corrosion inhibition. Scherrer equation was employed to calculate the crystallite size of the Ag-NPs. A larger crystallite size (33.564 nm) indicates a more stable and compact structure, which can enhance the protective properties of the NPs against corrosion. Conversely, smaller sizes (19.082 nm and 21.284 nm) may provide a higher surface area, potentially leading to enhanced adsorption and coverage on the mild steel surface.

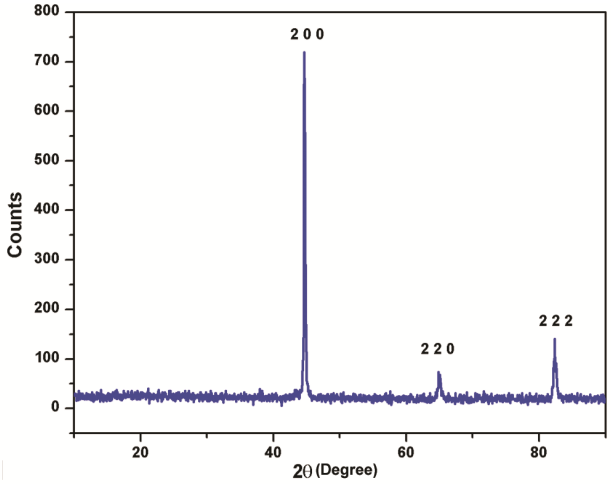


Fig. 1 — XRD Pattern of Thin Film deposited on MS Substrate of the Ag NPs

Table 1 — X-ray diffraction parameters of Ag-NPs deposited on mild steel substrate

| Parameters | Peak 1 | Peak 2 | Peak 3 | Average |
|---|---|---|---|---|
| Crystal Size (nm) | 33.564 | 19.082 | 21.284 | 24.643 |
| d (Spacing) | 2.024 | 1.434 | 1.170 | 1.542 |
| Dislocation Density ($nm^{-2}$) | 0.887 | 2.746 | 2.207 | 1.946 |
| Strain | 3.660 | 12.663 | 11.380 | 9.234 |

The *d*-spacing parameter, representing the distance between crystal planes, is directly related to the surface coverage and interfacial interaction of the NPs with the mild steel substrate. A greater *d*-spacing value of 2.024 nm indicates an enhanced accessibility and reactivity of the surface, thereby promoting the adsorption of NPs onto the surface of mild steel and facilitating the creation of a protective barrier to counteract corrosion.

The dislocation density parameter is important for evaluating the defect structure of the Ag-NPs. A lower dislocation density (0.887 $nm^{-2}$) indicates a higher structural integrity and fewer defects, contributing to enhanced corrosion resistance. Higher dislocation densities (2.746 $nm^{-2}$ and 2.207 $nm^{-2}$) may

lead to increased vulnerability to localized corrosion due to the presence of more active sites for corrosion initiation.

Strain, another critical parameter, is related to the distortion within the crystal lattice of the Ag-NPS. Higher strain values (3.660, 12.663, and 11.380) can introduce additional strain energy, potentially affecting the stability and adhesion of the NPs on the mild steel surface. Lower strain values are desirable for improved corrosion inhibition.

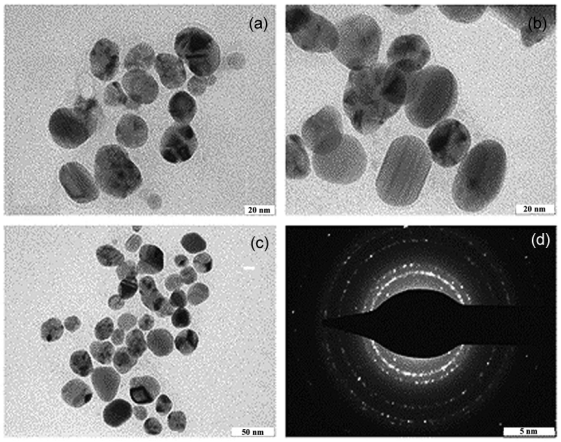


Fig. 2 — (a-c) TEM images at different resolutions and (d) SAED pattern of Ag-NPs

***Morphology of Ag-NPs***

TEM images of Ag-NPs are shown in Fig. 2(a-c). The images showed that although the Ag-NPs are non-uniform in size, ranging from 10 to 50 nm, they primarily have nearly spherical shape. The Ag-NPs were found to be surrounded by a weak, thin coating of other substances, which was probably caused by the capping organic substances made from *Nicotiana tabacum* leaf extract.

Additionally, as shown in Fig. 2d, the selected area electron diffraction (SAED) spots and ring-like diffraction patterns suggest that the NPs are polycrystalline in structure. These SAED spots are also roughly circular.

### *Surface Morphology*

The experimental substrate images of the mild steel coupons are depicted in Fig. 3. Fig. 3(a) demonstrates the initial surface morphology of the bare substrate, displaying a smooth and clean surface typical of the mild steel substrate with no experimental treatment performed. Fig. 3(b) shows a surface that is rougher, with visible cracks resulting from the exposure to a 3.5% NaCl solution. The presence of surface roughness, cracks, and pits indicates corrosion of the substrate in the solution.

Fig. 3(c) demonstrates a surface characterised by increased roughness and the presence of cracks,

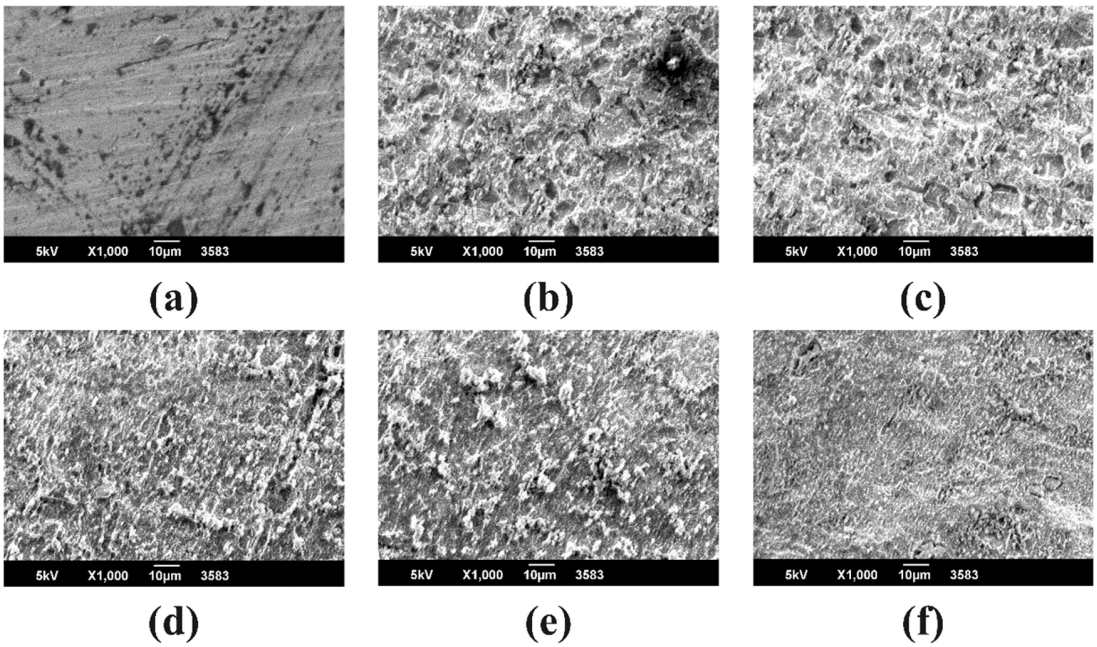


Fig. 3 — SEM Images of (a) bare substrate without any experimental treatment, (b) bare substrate subjected to experiments in a 3.5% NaCl solution, (c) bare substrate subjected to experiments in a 0.1 M HCl solution, (d) Ag-NPs deposited substrate without any experimental treatment, (e) Ag-NPs deposited substrate subjected to experiments in a 3.5% NaCl solution, and (f) Ag-NPs deposited substrate subjected to experiments in a 0.1 M HCl solution

overtaking the conditions observed in Fig. 3(b). This observation suggests a higher vulnerability of bare mild steel substrate to corrosion when exposed to a 3.5% NaCl solution as opposed to a 0.1 M HCl solution. The aforementioned observation finds corroboration in the polarisation data.

In Fig. 3(d), the visual representation showcases the deposition of Ag-NPs onto the substrate composed of mild steel. The observed luminous appearance of the substrate provides compelling evidence for the effective deposition of Ag-NPs onto its surface.

Fig. 3(e) showcases the experimental condition of the Ag-NPs-deposited substrate in a 3.5% NaCl medium, while Fig. 3(f) presents the examined surface in a 0.1 M HCl solution. Surface shown in Fig. 3(f) exhibits more pits and cracks compared to surface Fig. 3(e), which is consistent with the polarization data.

**Potentiodynamic Polarization Studies**

The investigation focused on examining the corrosion characteristics exhibited by a thin layer of Ag-NPs deposited onto a substrate composed of mild steel. The corrosive environments utilised for this study were solutions containing 3.5% NaCl and 0.1 M HCl. The Tafel polarisation curve technique was employed to analyse the corrosion behaviour. Fig. 4 shows the Tafel polarisation curve of Ag-NPs deposited on mild steel substrates. The polarization curve provides valuable insights into the corrosion characteristics and electrochemical response of the Ag-NPs-deposited substrate in different corrosive environments.

The electrochemical parameters pertaining to the aforementioned Tafel plots have been provided in Table 2, which shows the electrochemical parameters acquired for various deposition methodologies in 0.1 M HCl and 3.5% NaCl solutions, thereby offering significant elucidation pertaining to corrosion inhibition.

For bare substrate in 0.1M HCl, a corrosion potential ($E_{corr}$) of -295.08 mV was observed, accompanied by a corresponding corrosion current ($I_{corr}$) of 3.18 µA. The cathodic Tafel slope ($\beta_c$) was found to be $3.01974\times10^3$ V/decade, while the anodic Tafel slope ($\beta_a$) was $-2.6687\times10^3$ V/decade. The polarization resistance ($R_p$) was $-3.1348\times10^3$ Ohm.cm$^2$, and the corrosion rate ($C_R$) was $0.014\times10^2$ mm/year.

In a case involving the deposition of Ag-NPs in a solution of 0.1 M HCl, it was observed that the corrosion potential ($E_{corr}$) experienced a shift towards a higher positive value of 87.75 mV. This shift signifies an enhancement in the resistance to corrosion. The corrosion current ($I_{corr}$) significantly reduced to 0.182 µA, reflecting a lower tendency for corrosion. The cathodic Tafel slope ($\beta_c$) was $2.8526\times10^3$ V/decade, while the anodic Tafel slope ($\beta_a$) was $-1.9397\times10^3$ V/decade. The polarization resistance ($R_p$) increased to $-1.4462\times10^4$ Ohm.cm$^2$, indicating enhanced protection against corrosion. The corrosion rate ($C_R$) exhibited a notable decline to $0.0085\times10^2$ mm/year, while the corrosion efficiency

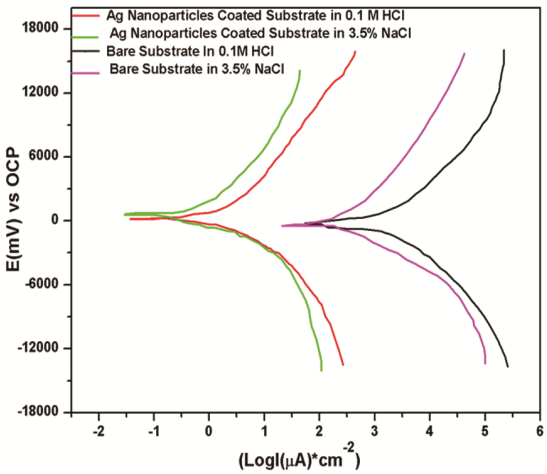


Fig. 4 — Tafel polarisation curve of silver nanoparticles deposited on mild steel substrates immersed in 3.5% sodium chloride (NaCl) and 0.1 M hydrochloric acid (HCl) solutions

Table 2 — Electrochemical parameters [Potential ($E_{corr}$), Current ($I_{corr}$), Anodic Tafel slope ($\beta_a$), Cathodic Tafel slope ($\beta_c$), Polarization Resistance ($R_p$), Corrosion Rate )($C_R$), and Corrosion Efficiency (PE)] pertaining to the corrosion inhibition of a mild steel substrate subjected to bare and Ag-NPs deposition, in solutions containing 0.1 M HCl and 3.5% NaCl

| Surface | Medium | $E_{corr}$ (mV) | $I_{corr}$ (µA) | $\beta_a$ (V/decade) | $\beta_c$ (V/decade) | $R_p$ (Ohm.cm$^2$) | $C_R$ (mm/year) | PE |
|---|---|---|---|---|---|---|---|---|
| Bare | 0.1 M HCl | -295.08 | 3.18 | $3.01\times10^3$ | $-2.67\times10^3$ | $-3.13\times10^3$ | $0.014\times10^2$ | - |
| Ag-NPs deposited | 0.1 M HCl | 87.75 | 0.182 | $2.85\times10^3$ | $-1.94\times10^3$ | $-1.45\times10^4$ | $0.008\times10^2$ | 94.27 |
| Bare | 3.5% NaCl | -590.16 | 2.464 | $7.88\times10^3$ | $-5.58\times10^3$ | $-3.37\times10^3$ | $0.011\times10^2$ | - |
| Ag-NPs deposited | 3.5% NaCl | -57.55 | 0.091 | $6.20\times10^3$ | $-5.84\times10^3$ | $-4.79\times10^4$ | $0.004\times10^2$ | 96.30 |

(PE) was ascertained to be 94.27%. These findings underscore the remarkable efficacy of the Ag-NPs in impeding corrosion within the 0.1 M HCl solution.

In a comparable manner, the bare substrate immersed in a solution containing 3.5% NaCl exhibited an observed $E_{corr}$ of -590.16 mV, associated with a $I_{corr}$ of 2.464 μA. The $\beta_c$ was determined to be 7.8776×103 V/decade, whereas $\beta_a$ exhibited a value of $-5.5790\times10^3$ V/decade. The $R_p$ was $-3.3693\times10^3$ Ohm $cm^2$, and $C_R$ was $0.0116\times10^2$ mm/year.

In contrast, Ag-NPs deposition in 3.5% NaCl led to a more positive $E_{corr}$ of -57.55 mV, indicating improved corrosion resistance. The $I_{corr}$ significantly reduced to 0.091 μA, demonstrating the effectiveness of the Ag-NPs in reducing corrosion. The $\beta_c$ was $6.2047\times10^3$ V/decade, while $\beta_a$ was $-5.8434\times10^3$ V/decade. The $R_p$ increased significantly to $-4.7887\times10^4$ Ohm.$cm^2$, indicating enhanced corrosion inhibition. The $C_R$ decreased to $0.0042\times10^2$ mm/year, and PE was determined to be 96.30%, highlighting the successful corrosion inhibition achieved by the Ag-NPs in the 3.5% NaCl solution.

## Conclusion

This study successfully achieved the green synthesis of Ag-NPs using *Nicotiana tabacum* leaf extract, producing crystalline particles with an average size of approximately 24 nm, as confirmed by XRD analysis. The environmentally friendly synthesis approach aligns with sustainability goals, offering a viable alternative to conventional nanoparticle production methods. Surface characterization revealed the uniform deposition of the silver nano-coating, and corrosion behaviour was systematically evaluated using the Tafel polarization method in 3.5% sodium chloride and 0.1 M hydrochloric acid solutions. The primary objective of developing an efficient anticorrosion coating was fulfilled, as the Ag-NPs demonstrated excellent corrosion inhibition efficiency. The results showed a significant reduction in corrosion rates, underscoring the superior protective performance of the silver nano-coating. These findings validate the potential of Ag-NPs as advanced corrosion inhibitors, particularly for mild steel in chloride-rich and acidic environments. Furthermore, the study highlights the applicability of silver nano-coatings in industrial scenarios requiring robust corrosion protection solutions. The findings of this research contribute to the development of cost-effective, durable, and environmentally friendly corrosion-resistant materials. Future research should focus on optimizing synthesis parameters, such as temperature, pH, and precursor concentration, to enhance nanoparticle size control, stability, and anticorrosive properties. Additionally, investigations into the long-term stability and durability of Ag-NPs-coated substrates in diverse environmental conditions are recommended. Future studies may include exposure to extreme temperatures, high humidity, and mechanical stresses to assess real-world performance.

## Acknowledgment

The author gratefully acknowledges the financial support provided by UGC-DAE CSR Indore, India under the CRS Project Scheme [Reference No. CSR-IC-MSRSR-06/CRS-214/2018-19]. Special thanks are extended to Dr. D. M. Phase, Director, UGC-DAE Consortium Indore Center, for granting permission to utilize the characterization techniques at the UGC-DAE Indore center. The authors also express gratitude to Dr. Mukul Gupta for conducting XRD characterization of the thin film at the UGC-DAE Indore center. Additionally, the authors acknowledge the assistance and expertise of Dr. R. Venkatesh and Mohan Gangrade in the Laser Confocal microscopy characterization technique, as well as their technical support at the UGC-DAE Indore Center.

## References

1 Sukarto A & Rochman N T, Effect of pH variation on particle size and purity of nano zinc oxide synthesized by sol-gel method, *Mater Sci J*, 12 (2012) 5.

2 Farag A A, Applications of nanomaterials in corrosion protection coatings and inhibitors, *Corros Rev*, 9 (2020) 189.

3 Joseph A, John-Mathew K P & Vandana S, Zirconium-doped ceria nanoparticles as anticorrosion pigments in waterborne epoxy–polymer coatings, *ACS Appl Nano Mater*, 4 (2020) 834.

4 Jain P, Patidar B & Bhawsar J, Potential of nanoparticles as a corrosion inhibitor: A Review, *J Bio Tribo Corros*, 6 (2020) 43.

5 Hasanin M S, Environmentally benign corrosion inhibitors based on cellulose niacin nano-composite for corrosion of copper in sodium chloride solutions, *Int J Biol Macromol*, 161 (2020) 345.

6 Peter A, Sharma S & Obot I, Anticorrosive efficacy and adsorptive study of guar gum with mild steel in acidic medium, *J Anal Sci Technol*, 7 (2016) 26.

7 Ikechukwu E E, Pauline E O, Ikechukwu E E & Pauline E O, Environmental impacts of corrosion on the physical properties of copper and aluminium: A case study of the surrounding water bodies in port harcourt, *Open J Soc Sci*, 03 (2015)143.

8 Gurrappa I & Malakondaiah G, Effect of environment on corrosion characteristics of newly developed DMR-1700 structural steel, *Sci Technol Adv Mater*, 9 (2008) 25005.
9 Koch G, Cost of corrosion, Trends in Oil and Gas Corrosion Research and Technologies*, Product Trans*, (2017) 3.
10 Abu-Thabit N Y & Makhlouf A S H, Recent advances in nanocomposite coatings for corrosion protection applications, *Handbook of Nanoceramic & Nanocomposite Coatings Materials*, Chapter-24 (2015) 515.
11 Borisova D, Möhwald H & Shchukin D G, Mesoporous silica nanoparticles for active corrosion protection, *ACS Nano*, 5 (2011) 1939.
12 Sharma S K, Jain G, Sharma J & Mudhoo A, Corrosion inhibition behaviour of *Azardirachta indica* (Neem) leaves extract as a green corrosion inhibitor for zinc in hydrochloric acid: A preliminary study, *Int J Appl Chem*, 6 (2010) 83.
13 Hooda A, Goyat M S, Gupta R, Prateek M, Agrawal M & Biswas A, Synthesis of nano-textured polystyrene/ZnO coatings with excellent transparency and superhydrophobicity, *Mater Chem Phys*, 193 (2017) 447.
14 Al-Ghanbusi B G B, Synthesis of aluminium oxide nanoparticles from waste aluminium foils for corrosion inhibition of mild steel pipe, *Indian J Chem Technol*, 31 (2024) 233.
15 Lu X, 3D reconstruction of plasma electrolytic oxidation coatings on Mg alloy via synchrotron radiation tomography, *Corros Sci*, 139 (2018) 395.
16 Bhawsar J, Jain P K & Jain P, Experimental and computational studies of Nicotiana tabacum leaves extract as green corrosion inhibitor for mild steel in acidic medium, *Alex Eng J*, 54 (2015) 769.
17 Ibrahim H M M, Green synthesis and characterization of silver nanoparticles using banana peel extract and their antimicrobial activity against representative microorganisms, *J Radiat Res Appl Sci*, 8 (2015) 265.
18 Vigneshwaran N, Nachane R P, Balasubramanya R H & Varadarajan P V, A novel one-pot 'green' synthesis of stable silver nanoparticles using soluble starch, *Carbohydr Res*, 341 (2006) 2012.
19 Paddock S W, Confocal laser scanning microscopy, *Biotechniques*, 27 (1999) 992.
20 Salaheldin T A, Husseiny S M, Al-Enizi A M, Elzatahry A & Cowley A H, Evaluation of the cytotoxic behavior of fungal extracellular synthesized Ag nanoparticles using confocal laser scanning microscope, *Int J Mol Sci*, 17 (2016) 329.
21 Mehta B K, Chhajlani M & Shrivastava B D, Green synthesis of silver nanoparticles and their characterization by XRD, *J Phys Conf Ser*, 836 (2017) 012050.